

RESEARCH PAPER

## Microwave-Assisted Synthesis of Alumina Nanoparticles Using Some Plants Extracts

Meisam Hasanpoor, Houman Fakhr Nabavi and Mahmood Aliofkhaezrai\*

Department of Materials Science, Faculty of Engineering, Tarbiat Modares University, Tehran, Iran

### ARTICLE INFO

#### Article History:

Received 14 October 2016

Accepted 12 December 2016

Published 01 January 2017

#### Keywords:

$Al_2O_3$

Chemical preparation

Microwave processing

Nanoparticle

### ABSTRACT

In present study we used five green plants for microwave assisted synthesis of Alumina nanoparticles from Aluminum nitrate. Structural characterization was studied using x-ray diffraction that showed semi- crystalline and possibly, amorphous structure. Fourier infrared spectroscopy was used to determine Al-O bond and functional groups responsible for synthesis of nanoparticles. FTIR confirmed existence of Al-O band and bio-functional groups, originated from plant extract. Morphology and size of nanoparticles were investigated using scanning electron microscopy, transmission electron microscopy and atomic force microscopy techniques. It was observed that nanoparticles have near-spherical shape. Average size of clusters of nanoparticles varied with different routes from of 60 nm to 300 nm. AFM images showed that Individual nanoparticles were less than 10 nm.

#### How to cite this article

Hasanpoor M, Fakhr Nabavi H, Aliofkhaezrai M. Microwave-Assisted Synthesis of Alumina Nanoparticles Using Some Plants Extracts. J Nanostruct, 2017; 7(1):1-7. DOI: 10.22052/jns.2017.01.005

### INTRODUCTION

Nanoparticles are synthesized with various methods; each of them provides a certain level of controllability of properties such as: structure, morphology and purity. Synthesis methods can be categorized in to three main parts as follows: Liquid phase methods, gas phase synthesis and methods basing on surface growth under vacuum conditions [1].

Cunha et al. [2], utilized sol gel method with natural organic matter to produce Alumina particles of diameter 52nm  $\pm$ 1. Toshio Itoh et al. [3], prepared  $\gamma$ - $Al_2O_3$  with polyol method using PVP. Optimized amount for reflux temperature and PVP molecular weight was investigated to control particles' size.  $\gamma$ - $Al_2O_3$  with particles size of 142 nm to 1.0 $\mu$ m was successfully synthesized and  $\alpha$ - $Al_2O_3$  was produced with subsequent annealing. Tahmasebpour et al. [4], investigated polyacrylamide sol-gel method to produce  $\alpha$ - $Al_2O_3$  nanoparticles. They found that

with low heating rates, phase transformation is delayed and as a consequence finer particles are resulted. It was also revealed that, particle size is independent of solution concentration. Zaki et al. [5, 6], used pechini method, a modified sol-gel method, to develop  $\alpha$ - $Al_2O_3$  nanoparticles. The main disadvantage of these conventional methods is long duration of preparation or reaction time, which is rectified by new developed methods such as microwave hydrothermal assisted synthesis. Microwave radiation can be used as a powerful heat source for synthesis of nanoparticles from liquid phase in short time.

Kiranmala Laishram et al. [7], Developed a combustive method for synthesis of  $\alpha$ - $Al_2O_3$  via microwave heating. In their experiment Aluminum nitrate and urea, prepared 1:2.5ratios, were dissolved in D/W to form a clear solution and subsequently heated with 900W for 3-5 minutes. After evaporation of the water, urea acts as a fuel and subsequent combustion synthesizes the

\* Corresponding Author Email: khazraei@modares.ac.ir

Alumina nanoparticles. Nanoparticles of 18-20 nm were produced which is comparable to peer practices such as low-temperature combustion synthesis. No calcination needed for  $\alpha$  to  $\gamma$  phase transformation. Leyla Sharifi et al. [8], investigated sol-gel microwave synthesis of Aluminum nitrate with microwave irradiation. They prepared gel from bohemite sol and dried gel was calcined in microwave with 900W. They found that in short time heating, first  $\gamma$ - $\text{Al}_2\text{O}_3$  nucleates and by increasing the irradiation time, more  $\alpha$ - $\text{Al}_2\text{O}_3$  is produced. After 10 minutes of irradiation  $\alpha$ - $\text{Al}_2\text{O}_3$  is the dominant phase. Sutradhar et al.[9], used polyol components in plant extracts to synthesize Alumina nanoparticles. 50-200 nm particles were produced from tea and coffee and 200-400 nm particles were produced from triphala. Elimination of capping agent or stabilizer and using green routes lays foundation for biological usage of nanopowders.

In further studies in microwave assisted synthesis of nanoparticles, Sahu et al. [10], produced  $\text{LaAlO}_3$ , Ragupathi et al. [11], synthesized Nickel Aluminate with plant extract and  $\text{BaTiO}_3$  was prepared by Katsuki et al. [12]. Nano composites of nHAp (nano-hydroxyapatite)-alumina and alumina-zirconia were produced in researches by radha et al. [13], and Benavente et al. [14], respectively.

In present study, we used microwave irradiation, as a powerful source for heating and used green routes, to maximize the purity and minimize chemical impurities in the product. Microwave-assisted synthesis using green extracts have been studied previously by plant extracts such as coffee, tea and triphala [9], Sesame [11], Biophytum sensitivum [15], Aerva lanata [16], bamboo hemicelluloses and glucose [17], Euphorbia nivulia [18]. In current research few plant extracts are used as reducer, without stabilizer, and effect of plant type on size and morphology of nanoparticles is investigated.

## MATERIALS AND METHODS

### Extract preparation

*Syzygium aromaticum* [19], *Origanum vulgare* [20], *Origanum majorana* [21], *Theobroma cacao* [22] and *Cichorium intybus* [23] were selected based on preliminary studies. 20 gr of mentioned plants were mixed with 100 ml of deionized water and boiled for 2h. After cooling in ambient

Table 1. Labeling of nanoparticles

Plant type	label
<i>Syzygium aromaticum</i>	ALNP-1
<i>Origanum vulgare</i>	ALNP-2
<i>Origanum majorana</i>	ALNP-3
<i>Theobroma cacao</i>	ALNP-4
<i>Cichorium intybus</i>	ALNP-5

temperature, they were centrifuged for 10 minutes and washed subsequently. Plant extracts were stored in 20-25 °C. Alumina nanoparticles synthesized with mentioned plant extracts are labeled according to Table 1.

### Synthesize procedure

Aluminum nitrate (>98%, Daejung, South Korea) and plant extracts were mixed with 1:4 weight ratios and then stirred for 10 minutes at room temperature. 850W LG microwave model No: MS1040SM/00v with 2.45 GHz frequency was used as heat source and solution was irradiated for 10 minutes at 610W. Irradiated solutions were centrifuged and washed with ethanol and deionized water for 10 minutes. To reduce agglomeration, powders were dissolved in deionized water and treated by ultrasonic vibration with 150 W for 5 minutes.

### Characterization

X-ray Diffraction (XRD) measurements were recorded using a "XPRT" diffractometer with a  $\text{Co K}\alpha$  tube operating at 40 kV/40 mA and the "PROPORTIONAL Xe FILLED" detector. The data were collected in the range of 20–90° with a step size of 0.040 ° and counting time of 0.8 s. The XRD patterns were evaluated using the Joint Committee Powder Diffraction Standards (JCPDS) for the phase determination. The patterns were analyzed with "High score plus" program.

FTIR studies were recorded using "PerkinElmer-Frontier FT-IR", to specify extract bio-components involved in synthesis of nanoparticles and AL-O structure. The morphology and size of nanoparticles were investigated with scanning electron microscopy (SEM, Philips XL30) operating at 25 KV. In a complementary study; finest powder was also studied via transmission electron microscopy (TEM, Zeiss - EM10C - 80 KV). Morphology and shape of nanoparticles were also studied by ARA AFM model No.0101/A with non-contact mode of imaging.

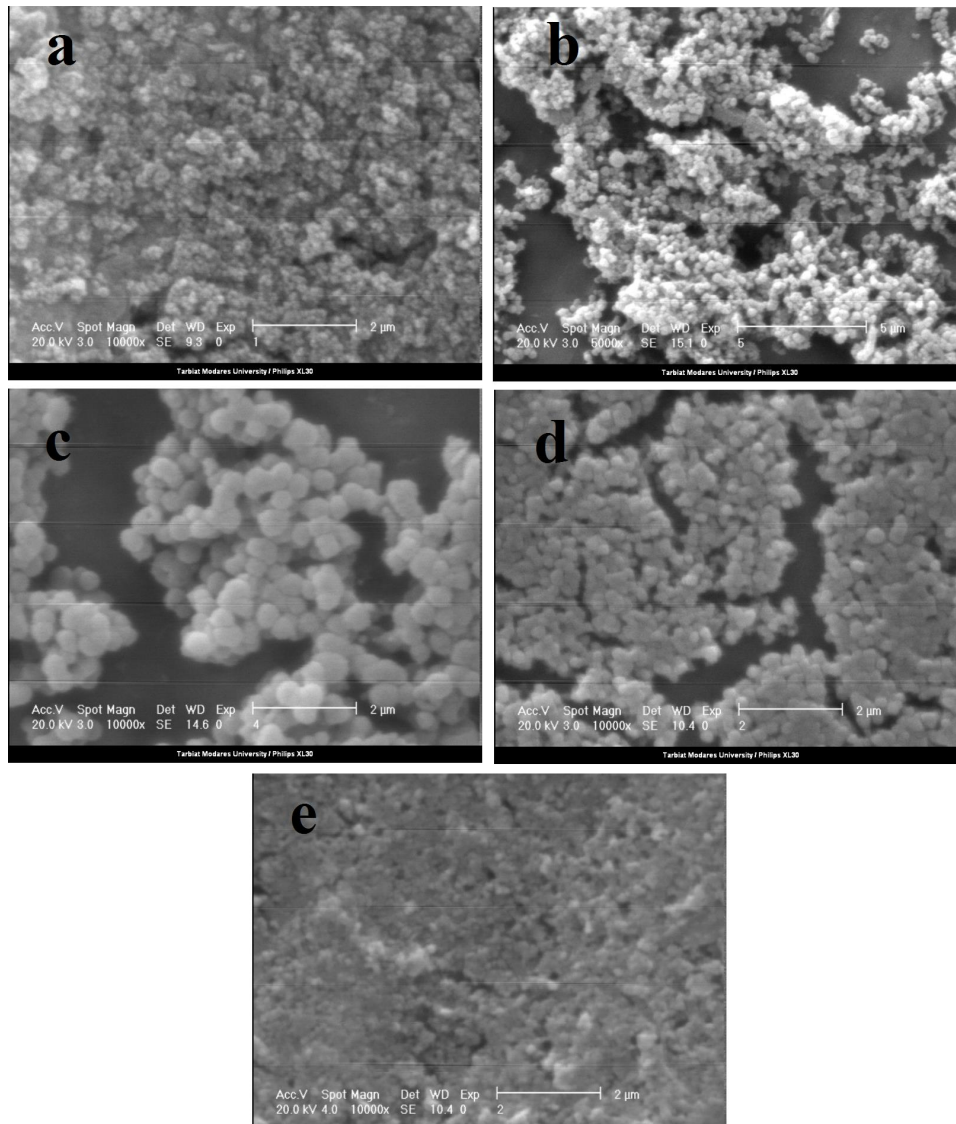


Fig 1. SEM image of a) ALNP-1 b) ALNP-2 c) ALNP-3 d) ALNP-4 e) ALNP-5

## RESULTS AND DISCUSSION

Fig. 1 shows SEM images of synthesized nanoparticles. All synthesized nanoparticles seem to have near spherical form. Nanoparticle clusters were between 60-300 nm. To investigate the size and morphology of nanoparticles more precisely, AFM and TEM analysis were applied. TEM image of ALNP-1 as an example (Fig. 2) revealed that nanoparticles are nearly spherical with 3-5 nm diameter, which was verified by the measured size of nanoparticles in AFM image (Fig. 3). Summarized measurement of size of all synthesized nanoparticles, using AFM analysis, is presented in table 2. It is obvious that nanoparticles are significantly smaller than the estimated dimensions from SEM images, which

may have roots in agglomeration of nanoparticles.

X-ray diffraction pattern of synthesized nanoparticles are presented in fig. 4. XRD of nanoparticles synthesized with *Syzygium aromaticum* extract is slightly different from others nanoparticles, which indicates poor crystalline structure [24]. According to Fig. 4, XRD pattern of

Table 2. Height of alumina nanoparticles measured with AFM analysis

Sample number	Average size (nm)
ALNP-1	8
ALNP-2	3
ALNP-3	5
ALNP-4	2
ALNP-5	9

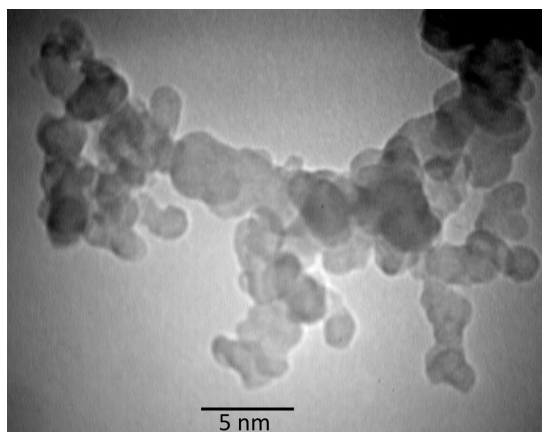


Fig 2. TEM image of ALNP-1

ALNP-1 has 3 characteristic peaks may be related with hexagonal corundum phase according to JCPDS card 96-900-9672. These significant peaks were detected at  $2\theta=40.99, 50.72, 67.80$ , correspond to (104), (113), (214) respectively. Broad peaks are indicative of very small crystalline size [25]. Crystalline size calculated according to Debye–Scherrer formula [26],  $d=0.89\lambda/\beta\cos\theta$ , where 'd' is the crystallite size and 0.89, Scherrer's constant,  $\lambda$ , the wavelength of X-rays.  $\theta$  is the Bragg diffraction angle, and  $\beta$ , the full width at half-maximum (FWHM) of the diffraction peak. Using the Debye–Scherrer's formula, crystalline size of nanopowders evaluated to be about 3-9 nm. XRD pattern of ALNP-3 might be assigned to cubic  $\text{Al}_2\text{O}_3$  with JCPDS card 01-075-0278. XRD pattern of other nanoparticles show no significant characteristic peak (Fig. 4). It may originate from being amorphous phase [27] or ultra-small particles of less than 5 nm [27, 28]. Moreover, It should be noted that distinguishing of amorphous and nanocrystalline structure is also dependent on line resolution which is determined by wavelength of X-ray radiation [29].

FTIR analysis was done to investigate Al-O bond and structural properties. Fig 5a illustrates FTIR spectroscopy of ALNP-1 nanoparticles. Alumina peaks are revealed from 467 to 922  $\text{cm}^{-1}$ . The band at 467  $\text{cm}^{-1}$  is assigned to  $\text{AlO}_6$  bending mode [5] and 580  $\text{cm}^{-1}$  is ascribed to asymmetric stretch of  $\text{AlO}_6$  [30]. Broad band at 638  $\text{cm}^{-1}$ , indicates  $\text{AlO}_6$  structure [7], and 759  $\text{cm}^{-1}$  peak is assigned to  $\text{AlO}_4$  symmetric stretching [30, 31]. 834 and 922  $\text{cm}^{-1}$  are possibly related to complex  $\text{AlO}_4$  and  $\text{AlO}_6$  interactive vibration [32]. Other peaks are located between 1000 and 1750  $\text{cm}^{-1}$ ,

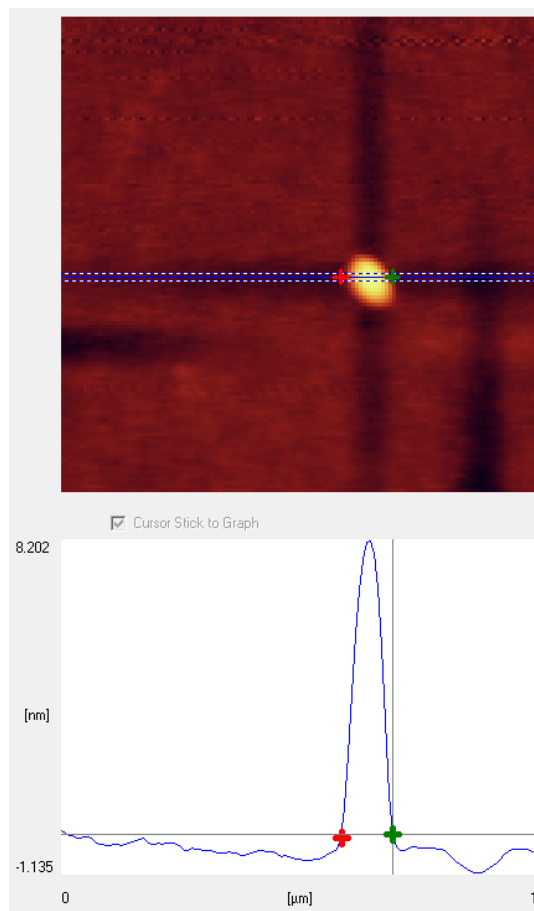


Fig 3. AFM image of ALNP-1

related to bio-functional groups originated from extract [15]. These groups are assumed to be flavonoids, tannins and terpenoids [19] attached to the nanoparticles and play an important role in synthesis and stabilization of nanoparticles [9, 15]. 1073  $\text{cm}^{-1}$  peak is related to C-N stretching frequency [9]. Peak located at 1200  $\text{cm}^{-1}$ , is possibly due to stretching vibration of Polyol [33]. 1376  $\text{cm}^{-1}$  peak is due to presence of geminal methyl group [9, 19]. 1590  $\text{cm}^{-1}$  peak could be assigned to adsorption of water [34, 35]. Peak located at 1446  $\text{cm}^{-1}$  is supposed to be originated from C–O–H in-plane bend of the hydroxyl groups [33]. Small band located at 1697  $\text{cm}^{-1}$  is possibly related to C=C aromatic ring [20]. FTIR of ALNP-2 is presented in Fig. 5b. Only one peak is related to alumina nanoparticles that is located at 609  $\text{cm}^{-1}$  and it is indicative of octahedron  $\text{AlO}_6$  only formation [5]. 1104  $\text{cm}^{-1}$  peak, is due to C–O–C stretching frequency and 1487  $\text{cm}^{-1}$  band is originated from Methylene group  $\text{CH}_2$  bending [36, 37] and finally, 1614  $\text{cm}^{-1}$

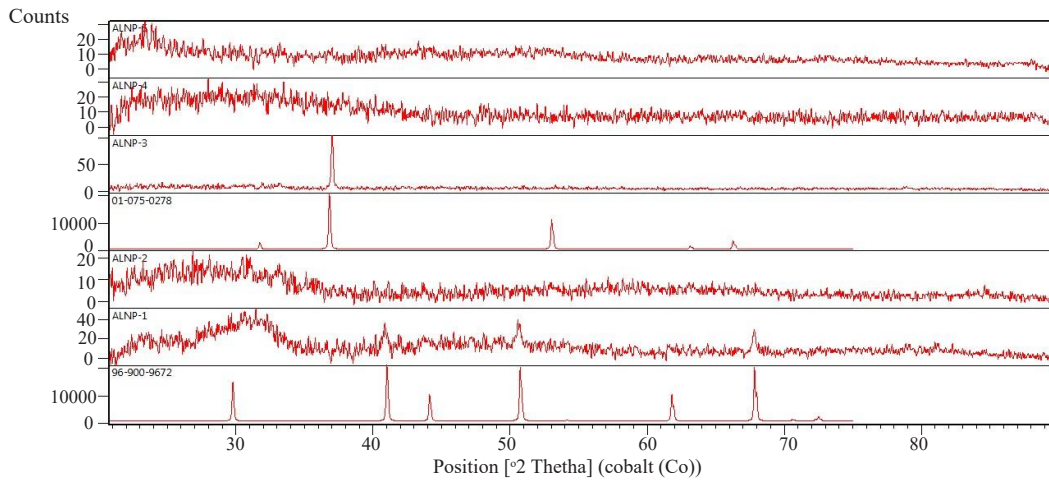


Fig 4. XRD pattern of Alumina nanoparticles

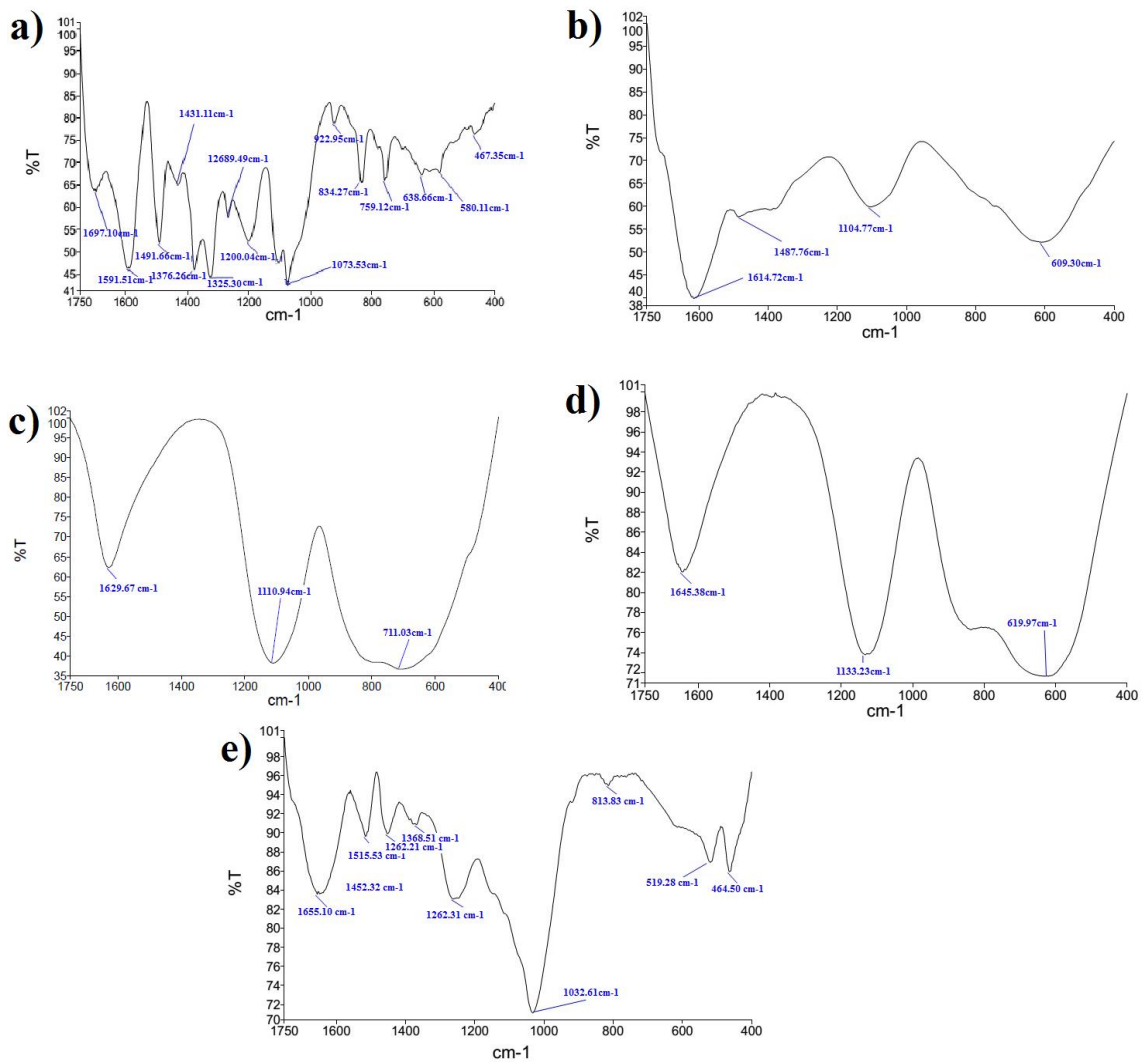


Fig 5. FTIR analysis of a) ALNP-1b) ALNP-2c) ALNP-3d) ALNP-4e) ALNP-5

suggests C=C aromatic bending [20]. Characteristic band of  $711\text{ cm}^{-1}$  in FTIR of ALNP-3 represents Al-O band (see Fig 5c). *Origanum majorana* extract contains Tannins, Flavonoids, Phenol compounds and Triterpenes [38]. Characteristic band of  $1110$  and  $1629$  may represent C-O stretch and aromatic ring respectively [22]. These peaks confirm presence of flavonones as adsorbed functional groups. FTIR of ALNP-4 is shown in Fig 5d, showing a broad band at  $619\text{ cm}^{-1}$  that is indicative of symmetric stretching of  $\text{AlO}_6$  [32]. The bands observed at  $1133$  and  $1645\text{ cm}^{-1}$  may be assigned to C-H or C-O stretch and C=C aromatic ring respectively [22]. Fig. 5e presents FTIR of ALNP-5.  $464$ ,  $519$  and  $813\text{ cm}^{-1}$  peaks are related to alumina nanoparticles. It can be suggested that both  $\text{AlO}_4$  and  $\text{AlO}_6$  were synthesized [39]. There are also broad and small bands around  $1000$  to  $1750\text{ cm}^{-1}$  which is indicative of bio-functional groups attached to the nanoparticles. Peaks located at  $1032\text{ cm}^{-1}$  may represent C-N band [9] and  $1262\text{ cm}^{-1}$  peak is ascribed to C-O band [22].  $1368$  and  $1452\text{ cm}^{-1}$  peaks may represent methyl and hydroxyl groups respectively [33]. There is a small band at  $1515\text{ cm}^{-1}$ , related to possible adsorption of water to surface [34, 35] and finally,  $1655\text{ cm}^{-1}$  broad band is indicative of aromatic ring [22].

## CONCLUSION

*Syzygium aromaticum*, *Origanum vulgare*, *Origanum majorana*, *Theobroma cacao* and *Cichorium intybus* were used as green routes for microwave assisted synthesis of alumina nanoparticles.

XRD pattern of particles synthesized with *Syzygium aromaticum* showed semi-crystalline structure while others showed no significant peak that might be assigned to nano dimension of particles or their amorphous structure.

FTIR studies of nanoparticles showed peaks in range of  $450$ - $1000\text{ cm}^{-1}$ , assigned to  $\text{AlO}_4$  and  $\text{AlO}_6$  bonds, and some peaks in range of  $1000$ - $1750\text{ cm}^{-1}$ : assigned to bio-functional groups responsible for particles synthesis.

SEM analysis of nanoparticles showed clusters of nanoparticles in  $60$ - $300\text{ nm}$  range. TEM and AFM analysis revealed that individual nanoparticles have less than  $10\text{ nm}$  size.

## CONFLICT OF INTEREST

The authors declare that there is no conflict of interests regarding the publication of this manuscript.

## REFERENCES

1. Kruijs FE, Fissan H, Peled A. Synthesis of nanoparticles in the gas phase for electronic, optical and magnetic applications—a review. *J Aerosol Sci.* 1998;29(5):511-35.
2. da Costa Cunha G, Romão LPC, Macedo ZS. Production of alpha-alumina nanoparticles using aquatic humic substances. *Powder Technol.* 2014;254(0):344-51.
3. Itoh T, Uchida T, Matsubara I, Izu N, Shin W, Miyazaki H, et al. Preparation of  $\gamma$ -alumina large grain particles with large specific surface area via polyol synthesis. *Ceram Int.* 2015;41(3, Part A):3631-8.
4. Tahmasebpour M, Babaluo AA, Shafiei S, Pipelzadeh E. Studies on the synthesis of  $\alpha$ - $\text{Al}_2\text{O}_3$  nanopowders by the polyacrylamide gel method. *Powder Technol.* 2009;191(1-2):91-7.
5. Zaki T, Kabel KI, Hassan H. Preparation of high pure  $\alpha$ - $\text{Al}_2\text{O}_3$  nanoparticles at low temperatures using Pechini method. *Ceram Int.* 2012;38(3):2021-6.
6. Zaki T, Kabel KI, Hassan H. Using modified Pechini method to synthesize  $\alpha$ - $\text{Al}_2\text{O}_3$  nanoparticles of high surface area. *Ceram Int.* 2012;38(6):4861-6.
7. Laishram K, Mann R, Malhan N. A novel microwave combustion approach for single step synthesis of  $\alpha$ - $\text{Al}_2\text{O}_3$  nanopowders. *Ceram Int.* 2012;38(2):1703-6.
8. Sharifi L, Beyhaghi M, Ebadzadeh T, Ghasemi E. Microwave-assisted sol-gel synthesis of alpha alumina nanopowder and study of the rheological behavior. *Ceram Int.* 2013;39(2):1227-32.
9. Sutradhar P, Debnath N, Saha M. Microwave-assisted rapid synthesis of alumina nanoparticles using tea, coffee and triphala extracts. *Adv Manuf.* 2013;1(4):357-61.
10. Sahu PK, Behera SK, Pratihari SK, Bhattacharyya S. Low temperature synthesis of microwave dielectric  $\text{LaAlO}_3$  nanoparticles: effect of chloride on phase evolution and morphology. *Ceram Int.* 2004;30(7):1231-5.
11. Ragupathi C, Vijaya JJ, Kennedy LJ. Preparation, characterization and catalytic properties of nickel aluminate nanoparticles: A comparison between conventional and microwave method. *J Saudi Chem Soc.* (0). Available from <http://dx.doi.org/10.1016/j.jscs.2014.01.006> ( Accessed 11 February 2014)
12. Katsuki H, Furuta S, Komarneni S. Semi-continuous and fast synthesis of nanophase cubic  $\text{BaTiO}_3$  using a single-mode home-built microwave reactor. *Mater Lett.* 2012;83(0):8-10.
13. Radha G, Balakumar S, Venkatesan B, Vellaichamy E. Evaluation of hemocompatibility and in vitro immersion on microwave-assisted hydroxyapatite-alumina nanocomposites. *Mater Sci Eng, C.* 2015;50(0):143-50.
14. Benavente R, Salvador MD, Penaranda-Foix FL, Pallone E, Borrell A. Mechanical properties and microstructural evolution of alumina-zirconia nanocomposites by microwave sintering. *Ceram Int.* 2014;40(7, Part B):11291-7.
15. Joseph S, Mathew B. Microwave-assisted green synthesis of silver nanoparticles and the study on catalytic activity in the degradation of dyes. *J Mol Liq.* 2015;204(0):184-91.

16. Joseph S, Mathew B. Microwave assisted facile green synthesis of silver and gold nanocatalysts using the leaf extract of *Aerva lanata*. *Spectrochim Acta, Part A*. 2015;136, Part C(0):1371-9.
17. Peng H, Yang A, Xiong J. Green, microwave-assisted synthesis of silver nanoparticles using bamboo hemicelluloses and glucose in an aqueous medium. *Carbohydr Polym*. 2013;91(1):348-55.
18. Valodkar M, Nagar PS, Jadeja RN, Thounaojam MC, Devkar RV, Thakore S. Euphorbiaceae latex induced green synthesis of non-cytotoxic metallic nanoparticle solutions: A rational approach to antimicrobial applications. *Colloids Surf, A*. 2011;384(1-3):337-44.
19. Raghunandan D, Bedre MD, Basavaraja S, Sawle B, Manjunath SY, Venkataraman A. Rapid biosynthesis of irregular shaped gold nanoparticles from macerated aqueous extracellular dried clove buds (*Syzygium aromaticum*) solution. *Colloids Surf, B*. 2010;79(1):235-40.
20. Sankar R, Karthik A, Prabu A, Karthik S, Shivashangari KS, Ravikumar V. *Origanum vulgare* mediated biosynthesis of silver nanoparticles for its antibacterial and anticancer activity. *Colloids Surf, B*. 2013;108(0):80-4.
21. Vera RR, Chane-Ming J. Chemical composition of the essential oil of marjoram (*Origanum majorana* L.) from Reunion Island. *Food Chem*. 1999;66(2):143-5.
22. Nasrollahzadeh M, Sajadi SM, Rostami-Vartooni A, Bagherzadeh M. Green synthesis of Pd/CuO nanoparticles by *Theobroma cacao* L. seeds extract and their catalytic performance for the reduction of 4-nitrophenol and phosphine-free Heck coupling reaction under aerobic conditions. *J Colloid Interface Sci*. 2015;448(0):106-13.
23. Bharathi K, Thirumurugan V, Kavitha M, Muruganadam G, Ravichandran K, Seturaman M. A comparative study on the green biosynthesis silver nano particles using dried leaves of *boerhaavia diffusa* L. And *cichorium intybus* L. With reference to their antimicrobial potential. *World J Pharmaceut Sci*. 2014;3(5):1415-27.
24. Li X, Guo X, Liu T, Zheng X, Bai J. Shape-controlled synthesis of Fe nanostructures and their enhanced microwave absorption properties at L-band. *Mater Res Bull*. 2014;59(0):137-41.
25. La Porta FA, Ferrer MM, De Santana YV, Raubach CW, Longo VM, Sambrano JR, et al. Synthesis of wurtzite ZnS nanoparticles using the microwave assisted solvothermal method. *J Alloys Compd*. 2013;556:153-9.
26. Cullity BD, Stock SR. *Elements of X-ray Diffraction: 3rd edition*. Pearson; 2001.
27. Liao X, Zhu J, Zhong W, Chen H-Y. Synthesis of amorphous Fe<sub>2</sub>O<sub>3</sub> nanoparticles by microwave irradiation. *Mater Lett*. 2001;50(5-6):341-6.
28. Van Hoang V, Ganguli D. Amorphous nanoparticles—Experiments and computer simulations. *Phys Rep*. 2012;518(3):81-140.
29. Machala L, Zboril R, Gedanken A. Amorphous Iron (III) Oxide A Review. *J Phys Chem B*. 2007;111(16):4003-18.
30. Sivadasan A, Selvam IP, Potty SN. Microwave assisted hydrolysis of aluminium metal and preparation of high surface area  $\gamma$ -Al<sub>2</sub>O<sub>3</sub> powder. *Bull Mater Sci*. 2010;33(6):737-40.
31. Boumaza A, Favaro L, Lédion J, Sattonnay G, Brubach JB, Berthet P, et al. Transition alumina phases induced by heat treatment of boehmite: An X-ray diffraction and infrared spectroscopy study. *J Solid State Chem*. 2009;182(5):1171-6.
32. Saniger J. Al-O infrared vibrational frequencies of  $\gamma$ -alumina. *Mater Lett*. 1995;22(1-2):109-13.
33. Aromal SA, Philip D. Benincasa hispida seed mediated green synthesis of gold nanoparticles and its optical nonlinearity. *Physica E*. 2012;44(7-8):1329-34.
34. Sankar KV, Senthilkumar ST, Berchmans LJ, Sanjeeviraja C, Selvan RK. Effect of reaction time on the synthesis and electrochemical properties of Mn<sub>3</sub>O<sub>4</sub> nanoparticles by microwave assisted reflux method. *Appl Surf Sci*. 2012;259(0):624-30.
35. Goharshadi EK, Hadadian M. Effect of calcination temperature on structural, vibrational, optical, and rheological properties of zirconia nanoparticles. *Ceram Int*. 2012;38(3):1771-7.
36. Hosseini SF, Zandi M, Rezaei M, Farahmandghavi F. Two-step method for encapsulation of oregano essential oil in chitosan nanoparticles: Preparation, characterization and in vitro release study. *Carbohydr Polym*. 2013;95(1):50-6.
37. Coates J. Interpretation of infrared spectra, a practical approach. *Enc Anal Chem*. 2000. Available from: 10.1002/9780470027318.a5606. (Accessed 15 SEP 2006)
38. Nowak K, Ogonowski J. Olejek majerankowy, jego charakterystyka i zastosowanie. *Chemik*. 2010;64(7-8):539-48.
39. Rinaldi R, Schuchardt U. On the paradox of transition metal-free alumina-catalyzed epoxidation with aqueous hydrogen peroxide. *J Catal*. 2005;236(2):335-45.